Journal of Alloys and Compounds 507 (2010) L43–L46

Contents lists available at ScienceDirect

Journal of Alloys and Compounds

journal homepage: www.elsevier.com/locate/jallcom

Letter

# Fabrication and photocatalytic property of α-$Bi_2O_3$ nanoparticles by femtosecond laser ablation in liquid

Geng Lin[a,b,*], Dezhi Tan[c], Fangfang Luo[a,b], Danping Chen[a], Quanzhong Zhao[a,*], Jianrong Qiu[d,*], Zhizhan Xu[a,*]

[a] State Key Laboratory of High Field Laser Physics, Shanghai Institute of Optics and Fine Mechanics, Chinese Academy of Sciences, Shanghai 201800, China
[b] Graduate School of the Chinese Academy of Sciences, Beijing 100039, China
[c] State Key Laboratory of Silicon Materials, Zhejiang University, Hangzhou 310027, China
[d] Key Lab of Specially Functional Materials of Ministry of Education, and Institute of Optical Communication Materials, South China University of Technology, Guangzhou 510641, China

ARTICLE INFO

*Article history:*
Received 2 June 2010
Received in revised form 4 August 2010
Accepted 4 August 2010
Available online 11 August 2010

*Keywords:*
Femtosecond laser ablation
α-$Bi_2O_3$ nanoparticle
Photocatalyst

ABSTRACT

α-$Bi_2O_3$ nanoparticles have been produced by femtosecond laser ablation in ethanol at room temperature. Their crystal structure, crystal phase, shape and size distribution, and photophysical property are investigated using X-ray diffraction, Raman, transmission electron microscopy (TEM), high-resolution TEM and UV–vis spectroscopy. The α-$Bi_2O_3$ nanoparticles produced by laser ablation with two particle size population distributions having the mean particle size of ~10 and ~60 nm exhibited a good photocatalytic activity on the photodegradation of indigo carmine under 365 nm light emitting diode irradiation.



## 1. Introduction

Over the past decade, a new photocatalyst bismuth oxide attracted increasing attention of their promising candidate for the visible light-activated photocatalyst due to their following advantages: (i) $Bi_2O_3$ with band gaps varying from 2 to 3.96 eV has optical absorption in the visible region [1–3]. (ii) Its intrinsic polarizabilities are favorable for the separation of photo-generated electron–hole pairs and the transfer of these charge carriers [4]. (iii) Its wide delocalized bands are beneficial to the diffusion of photo-generated charge carriers [5,6]. Thus, different types of $Bi_2O_3$ such as nanoparticles, nanofibers, thin films have been developed for studying their photocatalytic characteristics. It is known that, if the grain sizes of photocatalyst are reduced from micro-size to nano-size, the catalytic activities can be dramatically increased [7–9]. Hence preparation of nanostructured $Bi_2O_3$ photocatalysts doubtless deserves to be taken into account in future research. In recent years, laser ablation of a solid target in a liquid environment has been widely used in the synthesis of nanocrystals and fabrication of nanostructures due to the following advantages: (i) a chemically "simple and clean" synthesis [10–12], (ii) an ambient conditions not extreme temperature and pressure [13–15], (iii) the new phase formation of nanocrystals may involve in both liquid and solid [10], and (iv) structure, size, and shape of the synthesized nanocrystals can be controlled by tuning laser parameters and applied assistances [16–23]. Furthermore, compared with other normal laser ablation, femtosecond laser ablation has some advantages, such as higher temperature and higher pressure in a local volume can be achieved, higher temperature phase materials can be fabricated, and smaller nanocrystals with narrow size distribution can be obtained [10,12]. Therefore, in this letter, we reported the synthesis of $Bi_2O_3$ nanoparticles using a facile and rapid method of femtosecond pulsed laser ablation in liquid. And the photocatalytic properties of the obtained $Bi_2O_3$ nanoparticle were investigated.

## 2. Experimental

A typical experimental setup of pulsed laser ablation in liquid was shown in Fig. 1. First, the femtosecond laser was produced by a Ti/sapphire laser (Hurricane, Spectra Physics Lasers) with a wavelength of 800 nm, pulse width of 120 fs, repeating frequency of 1 kHz, and pulse energy of 0.5 mJ/pulse. Next, the bismuth oxide target with 99.8% purity which was pressed and sintered at 550 °C for 10 h was used as the starting material and fixed on the bottom of a quartz vessel which was put into an ultrasonic bath, and 99.9% ethanol was poured slowly into the vessel until the target was covered by about 10 mm. Finally, the pulse laser was focused on the surface of the target using a lens with a focal length of 100 mm. After the pulse laser interacted with the target for 60 min, the dark brown solution was collected before further

* Corresponding author at: State Key Laboratory of High Field Laser Physics, Shanghai Institute of Optics and Fine Mechanics, Chinese Academy of Sciences, Shanghai 201800, China.
*E-mail addresses:* xlin01@126.com (G. Lin), zqz@siom.ac.cn (Q. Zhao), qjr@zju.edu.cn (J. Qiu), zzxu@mail.shcnc.ac.cn (Z. Xu).

0925-8388/$ – see front matter. Crown Copyright © 2010 Published by Elsevier B.V. All rights reserved.
doi:10.1016/j.jallcom.2010.08.014

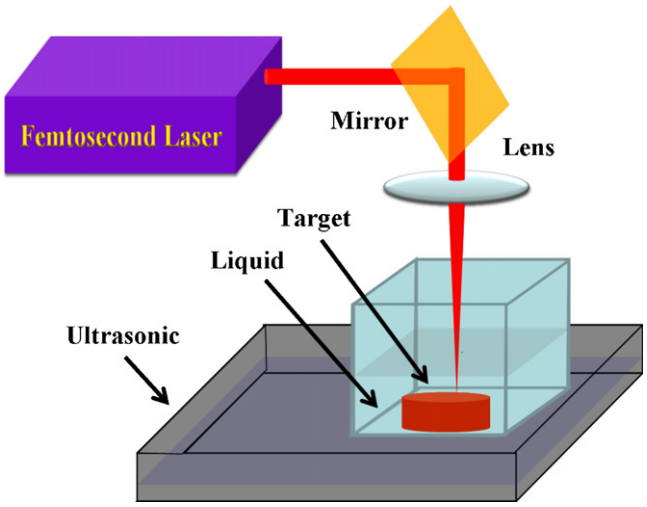


**Fig. 1.** Typical experimental setup for laser ablation in liquids.

measurements. The powder sample was collected after centrifugation at 7000 rpm and evaporating the solutions at 80 °C for 4 h. Raman spectra and X-ray diffraction (XRD) analysis were used to study the crystal phases of the sample. Raman spectra analysis was carried out with Labor Raman HR-800. The XRD measurement was performed using a Rigaku D/MAX-RA diffractometer with Cu $K_\alpha$ as the incident radiation source. Transmission electron microscopy (TEM) was used to study the shape and size distribution of the synthesized nanoparticles. High-resolution TEM (HRTEM) was used to analyze the crystal phases. (HR)TEM micrographs were recorded on JEM-2010 high-resolution transmission electron microscope. A small droplet of the liquid obtained after ablation was deposited onto a copper grid with carbon film for TEM and HRTEM analysis.

The photodegradation of indigo carmine was used to evaluate the photocatalytic activities of the $Bi_2O_3$ nanoparticle. Photocatalytic experiments were carried out in a transparent, colorless glass vessel. A commercial 365 nm LED was used as a light source, and fixed 10 cm away from the vessel. 50 mg of $Bi_2O_3$ nanoparticle was suspended in 100 mL of indigo carmine solution with a concentration of 20 mg/L under magnetic stirring. The reaction system was first kept in the dark for 60 min to establish an adsorption–desorption equilibrium, and then exposed to the light source. At the desired time intervals, 2 mL aliquot was taken, followed by centrifugation and filtration to remove the catalyst. The supernatant was used to determine the concentration of residual indigo carmine in solution. The decolorization was determined by measuring the change in its characteristic optical absorbance. Absorption spectra were recorded by a spectrophotometer (JASCO V-570).

## 3. Results and discussion

The power sample was obtained by evaporating the solutions at 80 °C for 4 h which was produced by femtosecond laser ablation bismuth oxide target in ethanol. Fig. 2 shows the XRD patterns of the sample. The pattern feature can be well indexed by the diffraction peaks of $Bi_2O_3$ (JCPDS No. 270053). This $Bi_2O_3$ (JCPDS No. 270053) has a monoclinic symmetry with a space group of $P2_1/c$. It is known that there exist five polymorphs of $Bi_2O_3$ which possess distinct crystalline structures and physical (electrical, optical, etc.) properties [24,25]. And the polymorphs strongly depend on the synthesis method. The $\alpha$-$Bi_2O_3$ is a stable low temperature polymorph, which is reported to be monoclinic. In our

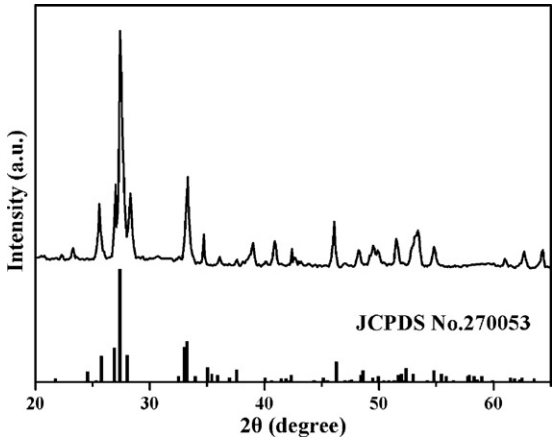


**Fig. 2.** XRD patterns of the $Bi_2O_3$ produced by femtosecond laser ablation.

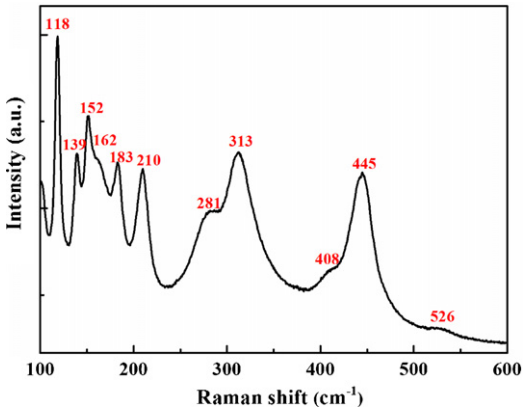


**Fig. 3.** Raman spectra of the $Bi_2O_3$ produced by femtosecond laser ablation.

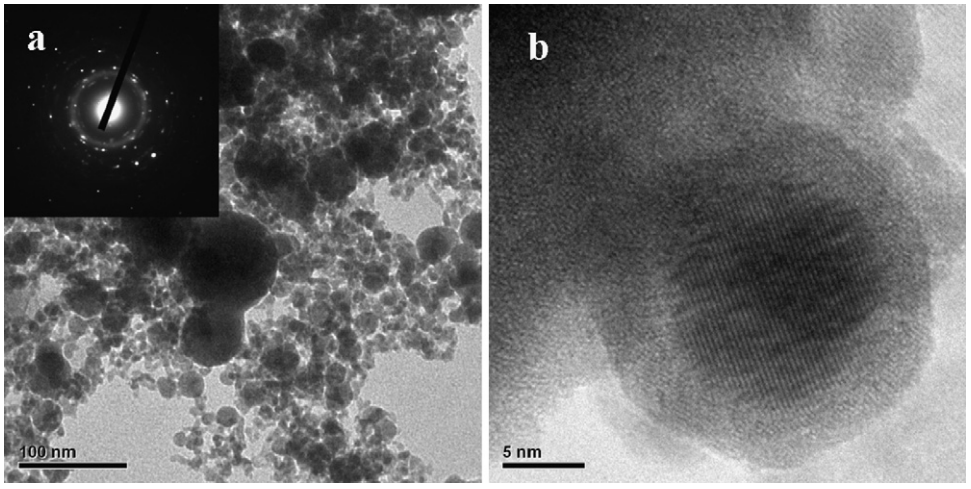


**Fig. 4.** (a) TEM (b) HRTEM images of the $Bi_2O_3$ nanoparticles produced by femtosecond laser ablation. The inset shows the SAED pattern.

case, the $Bi_2O_3$ produced by femtosecond laser ablation was α-$Bi_2O_3$.

Raman analysis was used to confirm the phase information of the $Bi_2O_3$ produced by femtosecond laser ablation. Fig. 3 presents the Raman spectrum of the $Bi_2O_3$. As shown in Fig. 3 the Raman peaks at 118, 139, 152, 162, 183, 210, 281, 313, 408, 445, and 526 nm are the characteristic bands of α-$Bi_2O_3$ [26]. The Raman result was consistent with the XRD result.

Detailed information about the shape of the α-$Bi_2O_3$ nanoparticles in the produced solutions was obtained by TEM. Fig. 4a shows that the particles are almost spherical or irregular spherical with two particle size population distributions having the mean particle size of ~10 and ~60 nm. Selected-area electron diffraction (SAED) pattern shown in the inset of Fig. 4a confirmed that the crystalline phase was monoclinic α-$Bi_2O_3$. High-resolution TEM imaging of the nanoparticles also revealed the crystalline structure. Fig. 4b shows the lattice interplanar spacing of α-$Bi_2O_3$ nanoparticles produced in ethanol was measured to be equal to 3.16 Å which corresponds to the crystallographic of (0 1 2) planes of the monoclinic α-$Bi_2O_3$. The size distribution of the $Bi_2O_3$ nanoparticle shows a bi-modal. Similar size distributions were reported by Link [27] and Inasawa [28]. They suggested this phenomenon was attributed to laser-induced size reduction of the large size nanoparticles followed by the formation of small particles. Laser-induced size reduction is a common phenomenon which has been reported by many researchers and its kinetic processes also have been extensively studied [27,28]. Therefore, we suggested the bi-modal distribution of $Bi_2O_3$ nanoparticle ablated by femtosecond laser was ascribed to laser-induced size reduction. Meanwhile, an energy-dispersive X-ray (EDX) spectrum within the measurement error of 2% was exhibited in Fig. 5, which clearly indicates that these nanoparticles were mainly composed of Bi (43.57%), and O (55.32%), with the supposed molecular formula $Bi_2O_{2.54}$. Thus, it was suggested that there are lots of oxygen deficient defects in these α-$Bi_2O_3$ nanoparticles. Additionally, the Cu, Cr, and Ca peaks were originated from the copper grid and amorphous carbon film support, respectively.

Fig. 6 indicates the absorption spectra of the solutions obtained by femtosecond laser ablation. The optical absorbance of an indirect band gap semiconductor near the band edge follows an equation of $(\alpha h\nu)^{1/2} = A(h\nu - E_g)$, where $\alpha$, $h$, $\nu$, $E_g$, and $A$ are the absorption coefficient, Planck constant, light frequency, band gap, and a constant, respectively [29]. The band gap of α-$Bi_2O_3$ was estimated to be about 3.38 eV by plotting $(\alpha h\nu)^{1/2}$ versus $h\nu$, which

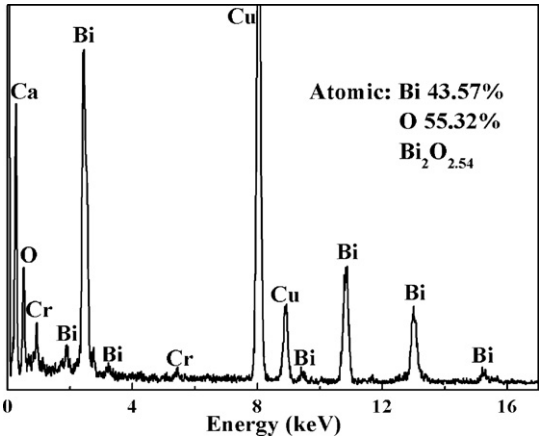


**Fig. 5.** EDX spectrum of the particles.

was higher than those previously reported values (2.3–2.9 eV) [2]. This could be explained by the so-called size quantization effect the first excited electronic state (the fundamental absorption edge) of a quantum dot is expected to show a shift to lower wavelengths (higher energies) with respect to the band gap absorption edge of the corresponding bulk material [30]. Fig. 4b shows the dependence of the absorbance of the α-$Bi_2O_3$ nanoparticle on the laser ablation time. The absorbance of the α-$Bi_2O_3$ nanoparticle rapidly increases with increasing laser ablation time which indicates that the pulsed laser ablation in liquid method is an efficient technology for producing α-$Bi_2O_3$ nanoparticles.

According to Refs. [10,12], we discussed the mechanism of the formation of nano α-$Bi_2O_3$ by femtosecond laser ablation as follows: pulsed laser ablation in liquid is a highly non-equilibrium process. When the ultra-short laser pulses irradiate the interface between the solid target and liquid through the liquid, the pulse energy can be released in a ultra-short time. Species will be ejected out with large kinetic energy after the laser irradiation and a plasma plume can be created on the interface. The plasma plume adiabatically expands quickly while the liquid confines it. The confinement of liquid could drive the plasma plume into an extreme thermodynamic state in which the temperature and pressure reach vary high. The species in the plume collided and react with molecules of the surrounding liquid and the materials will form in these extreme

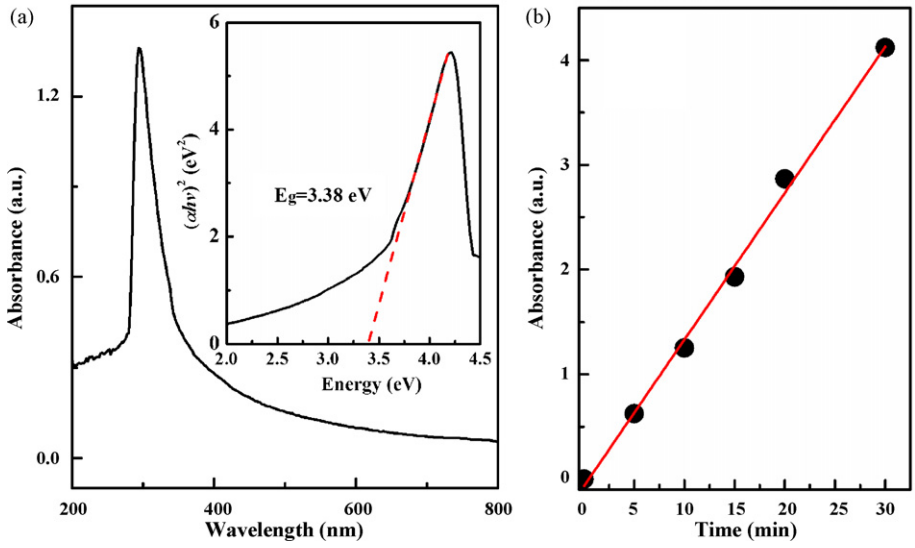


**Fig. 6.** (a) UV–vis absorbance spectra of the $Bi_2O_3$ solution obtained by femtosecond laser ablation, inset shows the plots of $(\alpha h\nu)^2$ versus energy $(h\nu)$ for the band gap energies. (b) The dependence of the absorbance of the $Bi_2O_3$ on the laser ablation time.

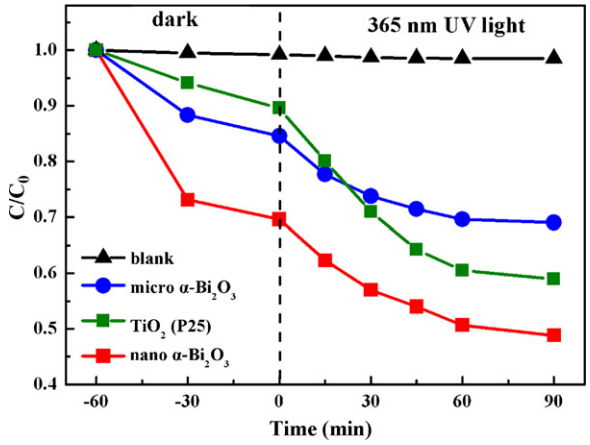


**Fig. 7.** Photodecomposition of indigo carmine in solution in the presence of various photocatalysts and without a photocatalyst. $C$ is the concentration of the indigo carmine at time $t$ and $C_0$ is the initial concentration.

states. Moreover, the cooling of liquid can lead to quenching of the plasma plume which freezes and preserves materials in the final products. In our case, species was ablated from the bismuth oxide target by femtosecond laser pulse and then nucleation and growth of nano $\alpha$-$Bi_2O_3$ was happened for the high temperature, and finally nano $\alpha$-$Bi_2O_3$ reserved after fast quenching of the plasma plume.

The photocatalytic activities of the $\alpha$-$Bi_2O_3$ nanoparticles were evaluated by photo-oxidation of aqueous indigo carmine. For comparison, pure micro-size $\alpha$-$Bi_2O_3$, and $TiO_2$ (P25) were chosen as the reference photocatalysts. Fig. 7 shows the photodegradation results of indigo carmine catalyzed by all the catalysts. In the absence of a photocatalyst, the indigo carmine solution was slowly photo-bleached. It can be seen that the degradation efficiency by micro-size $Bi_2O_3$ was low owing to less-defect crystal structure. On the contrary, the nano-size $\alpha$-$Bi_2O_3$ shows a strong adsorptive capacities and comparable photocatalytic activities, which were much better than micro-size $\alpha$-$Bi_2O_3$ and $TiO_2$ (P25). It is known that, if the grain sizes of photocatalyst are reduced from micro-size to nano-size, the catalytic activities can be dramatically increased, which is owing to the larger surface-to-volume ratio and more defects of nano-size materials [7–9]. Generally, anionic dye of indigo carmine is readily adsorbed by oxides due to the plenty of positively charged defects on their surfaces [31]. As a result, the indigo carmine solution became pale and the $\alpha$-$Bi_2O_3$ nanoparticles turned light green when the photocatalytic system was kept in the dark for 60 min. Then the nanoparticles quickly recovered to its original yellow color under 365 nm UV light radiation, indicating that the photocatalytic process occurred over the surface of the $\alpha$-$Bi_2O_3$ nanoparticles. The solution became nearly colorless under further light irradiation. This result indicates that $\alpha$-$Bi_2O_3$ nanoparticles could be a good candidate to be exploited as a photocatalyst.

## 4. Conclusions

$\alpha$-$Bi_2O_3$ nanoparticles with two size population distributions having the mean particle size of ~10 and ~60 nm have been produced by femtosecond laser ablation in ethanol at room temperature. Due to the so-called size quantization effect, the band gap of $\alpha$-$Bi_2O_3$ was estimated to be about 3.38 eV, which was higher than those previously reported values. The $\alpha$-$Bi_2O_3$ nanoparticles exhibited a good photocatalytic activity on the photodegradation of indigo carmine under 365 nm light emitting diode irradiation.

## Acknowledgement

This work was financially supported by National Nature Science Foundation of China (Grant Nos. 50672087 and 60778039), National Basic Research Program of China (2006CB806007) and National High Technology Program of China (2006AA03Z304). This work was also supported by the program for Changjiang Scholars and Innovative Research Team in University (IRT0651).

## References

[1] F.I.V. Dolocan, Phys. Status Solidi A 64 (1981) 755.
[2] L. Leontie, M. Caraman, M. Delibas, G.I. Rusu, Mater. Res. Bull. 36 (2001) 1629.
[3] L. Leontie, M. Caraman, A. Visinoiu, G.I. Rusu, Thin Solid Films 473 (2005) 230.
[4] X. Lin, F. Huang, W. Wang, J. Shi, Scr. Mater. 56 (2007) 189.
[5] J. Tang, Z. Zou, J. Ye, J. Phys. Chem. C 111 (2007) 12779.
[6] A. Walsh, G.W. Watson, D.J. Payne, R.G. Edgell, J. Guo, P.A. Glans, T. Learmonth, K.E. Smith, Phys. Rev. B 73 (2006) 235104.
[7] L. Zhang, J. Lin, Z. Chen, Y. Tang, Y. Yu, Appl. Catal. A: Gen. 299 (2006) 292.
[8] J.C. Yu, J.G. Yu, W.K. Ho, L.Z. Zhang, Chem. Commun. (2001) 1942.
[9] T. Park, S.A. Haque, R.J. Potter, A.B. Holmes, J.R. Durrant, Chem. Commun. (2003) 2878.
[10] G.W. Yang, Prog. Mater. Sci. 52 (2007) 648.
[11] G.W. Yang, J.B. Wang, Q.X. Liu, J. Phys.: Condens. Matter 10 (1998) 7923.
[12] A. Amendola, M. Meneghetti, Phys. Chem. Chem. Phys. 11 (2009) 3805.
[13] F. Mafune, J. Kohno, Y. Takeda, T. Kondow, H. Sawabe, J. Phys. Chem. B 104 (2000) 9111.
[14] K. Anikin, N. Melnik, A. Simakin, G. Shafeev, V. Voronov, A. Vitukhnovsky, Chem. Phys. Lett. 366 (2002) 357.
[15] G. Compagnini, A.A. Scalisi, O. Puglisi, Phys. Chem. Chem. Phys. 4 (2002) 2787.
[16] D. Beena, K.J. Lethy, R. Vinodkumar, A.P. Detty, V.P. Mahadevan Pillai, V. Ganesan, J. Alloys Compd. 489 (2010) 215.
[17] K. Praveena, K. Sadhana, S.R. Murthy, J. Alloys Compd. 492 (2010) 245.
[18] D.S. Milovanović, B.B. Radak, B.M. Gaković, D. Batani, D. Miloš, M.D. Momčilović, M.S. Trtica, J. Alloys Compd. 501 (2010) 89.
[19] L. Yang, P.W. May, L. Yin, T.B. Scott, Nanotechnology 18 (2007) 215602.
[20] T. Asahi, T. Sugiyama, H. Masuhara, Acc. Chem. Res. 41 (2008) 1790.
[21] H. Cui, P. Liu, G.W. Yang, Appl. Phys. Lett. 89 (2006) 153124.
[22] P. Liu, Y.L. Cao, H. Cui, X.Y. Chen, G.W. Yang, Chem. Mater. 20 (2008) 494.
[23] P. Liu, Y.L. Cao, C.X. Wang, X.Y. Chen, G.W. Yang, Nano Lett. 8 (2008) 2570.
[24] S.N. Narang, N.D. Patel, V.B. Kartha, J. Mol. Struct. 327 (1994) 221.
[25] F.D. Hardcastle, I.E. Wachs, J. Solid State Chem. 97 (1992) 319.
[26] R.J. Betsch, W.B. White, Spectrochim. Acta 34A (1978) 505.
[27] S. Link, C. Burda, B. Nikoobakht, M.A. El-Sayed, J. Phys. Chem. B 104 (2004) 6152.
[28] S. Inasawa, M. Sugiyama, Y. Yamaguchi, J. Phys. Chem. B 109 (2005) 9404.
[29] M.A. Butler, J. Appl. Phys. 48 (1977) 1914.
[30] L.E. Brus, J. Chem. Phys. 80 (1984) 4403.
[31] Y. Wang, Y. Wen, H. Ding, Y. Shan, J. Mater. Sci. 45 (2010) 1385.